Biochemistry and Biophysics Reports 5 (2016) 448–452

Contents lists available at ScienceDirect

Biochemistry and Biophysics Reports

journal homepage: www.elsevier.com/locate/bbrep

Expression and production of soluble *Mycobacterium tuberculosis* H37Rv mycosin-3

Zhuo Fang [a,*], Wolf-Dieter Schubert [b], Nicolaas Claudius Gey van Pittius [a]

[a] DST/NRF Centre of Excellence in Biomedical Tuberculosis Research, US/MRC Centre for Molecular and Cellular Biology, Division of Molecular Biology and Human Genetics, Department of Biomedical Sciences, Faculty of Medicine and Health Sciences, University of Stellenbosch, Francie van Zijl Drive, Tygerberg 7505, South Africa

[b] Department of Biochemistry, University of Pretoria, cnr Lynnwood Road and Roper Street, Hatfield, Pretoria 0028, South Africa

ARTICLE INFO

Article history:
Received 15 December 2015
Received in revised form
3 February 2016
Accepted 4 February 2016
Available online 6 February 2016

Keywords:
Mycobacterium tuberculosis
ESX
Mycosin-3
Protein production
Cloning

ABSTRACT

Mycobacteria encode five type VII secretion system (T7SS) or ESX for nutrient acquisition and virulence. Mycosins are membrane-anchored components of ESX with serine protease activity but an unidentified substrate range. Establishing the substrate specificity of individual mycosins will help to elucidate individual ESX functions. Mycosin-1 and -3 orthologues from two environmental mycobacterial species, *Mycobacterium smegmatis* and *Mycobacterium thermoresistibile*, have been heterologously produced, but mycosins from *Mycobacterium tuberculosis* (*Mtb*) remain to be studied. Here we describe the successful production of *Mtb* mycosin-3 as a first step in investigating its structure and function.

1. Introduction

Pathogenic Gram negative bacteria use a range of secretion systems to secrete virulence factors or transport the factors into host cells to manipulate the host immune system [1]. Type VII secretion systems (T7SSs) are restricted to mycobacteria and some other high GC Gram-positive bacteria [2,3]. *Mycobacterium tuberculosis* (*Mtb*), the etiological agent of tuberculosis, has five T7SSs, denoted as ESX-1 to -5 presumably evolved by gene duplication [4]. ESX-1 and -5 are critical to virulence in pathogenic mycobacteria [5], and ESX-3 participates in mycobactin-mediated iron acquisition [6,7]. ESX-5 was recently found to additionally function in nutrient acquisition [8]. ESX-1, 3 and 5 are correspondingly essential for *Mtb* growth *in vitro* [9,10]. The roles of ESX-2 and -4 are not yet clear. The close association of ESXs with fundamental biological processes has resulted in much research interest in T7SS.

Details of T7SS secretion have not been fully elucidated including the highly conserved mycosin components. Analysing mycosins may therefore help to unravel their functions. Mycosin-5 was not co-isolated with the central, double membrane spanning complex consisting of EccB, EccC, EccD and EccE, indicating a weak association *in vivo* [11]. Mycosins share a conserved catalytic triad of aspartate, histidine and serine with subtilisin-like serine proteases [12]. Screening experiments, however, did not identify mycosin substrates [12]. Recently, mycosin-1 ($MycP_1$) was found to cleave EspB twice upon secretion [13] to potentially facilitate its maturation for host target interaction. This is, however, unlikely to be the only mycosin substrate, as the gene *espB* is unique to ESX-1. ESX-1 substrate secretion is dependent on mycosin-1 but removing its enzymatic activity unexpectedly increases secretion [13]. Mycosin-1 may thus ensure *Mtb* persistence by balancing immune detection and virulence [13].

Mycosins have an N-terminal secretion signal followed by a potential “pro-peptide”, a catalytic domain, a proline-rich linker and a hydrophobic transmembrane region (Fig. 1). While removal of the “pro-peptide” was originally proposed to be required for enzymatic activation [12], this was found not to affect its protease activity [14–16]. In addition, crystal structures of mycosin-1 from *M. smegmatis* and *M. thermoresistibile* and mycosin-3 ($MycP_3$) from *M. smegmatis* suggest that the “pro-peptide” wraps around the catalytic domain possibly to stabilize it. The “pro-peptide” has hence been renamed the “N-terminal extension region” [14–16]. The $MycP_1$ orthologue of *M. smegmatis* inefficiently cleaves EspB *in vitro* possibly due to other ESX-1 components being absent [14]. However, mycosin-1 orthologues from *M. smegmatis* and *M. thermorsistibile* are unlikely to be involved in virulence in these saprophytic species despite an amino acid sequence identity of 70% with *Mtb* protein. Production of recombinant mycosin-1 or -3 from *M. tuberculosis* is problematic. Although the role of mycosin-3 remains enigmatic, it is essential to *M. tuberculosis* survival *in vitro*

* Corresponding author.
E-mail addresses: zf@sun.ac.za (Z. Fang), wolf-dieter.schubert@up.ac.za (W.-D. Schubert), ngvp@sun.ac.za (N.C. Gey van Pittius).

http://dx.doi.org/10.1016/j.bbrep.2016.02.005

```
1-   MIRAAFACLAATVVVAGWWTPPAWAIGPPVVDAAAQPPSGDPGPVAPMEQRGACSVSGVI
61-  PGTDPGVPTPSQTMLNLPAAWQFSRGEGQLVAIIDTGVQPGPRLPNVDAGGDFVESTDGL
121- TDCDGHGTLVAGIVAGQPGNDGFSGVAPAARLLSIRAMSTKFSPRTSGGDPQLAQATLDV
181- AVLAGAIVHAADLGAKVINVSTITCLPADRMVDQAALGAAIRYAAVDKDAVIVAAAGNTG
241- ASGSVSASCDSNPLTDLSRPDDPRNWAGVTSVSIPSWWQPYVLSVASLTSAGQPSKFSMP
301- GPWVGIAAPGENIASVSNSGDGALANGLPDAHQKLVALSGTSYAAGYVSGVAALVRSRYP
361- GLNATEVVRRLTATAHRGARESSNIVGAGNLDAVAALTWQLPAEPGGGAAPAKPVADPPV
421- PAPKDTTPRNVAFAGAAALSVLVGLTAATVAIARRRREPTE
```

Fig. 1. The primary structure of *M. tuberculosis* mycosin-3 ($MycP_3$). Single underline: signal peptide; double underline: N-terminal extension; dashed underline: proline-rich linker; wave underline: hydrophobic transmembrane region; white on black: catalytic triad, Asp^{95}-His^{126}-Ser^{342}.

Table 1
Primers used to generate the starting *M. tuberculosis* $mycP_3$ construct (pET-28a construct was not codon-optimized), and eight codon-optimized $mycP_3$ constructs (Constructs A to I), Expression hosts and vectors are as listed.

Construct Name	Encoded Amino Acid Sequence	Expression Host	Expression Vector	Primer Sequences and Their Restriction Sites
Construct A	Ile^{26}-Asn^{430}	*E. coli* BL21 (DE3) pLysS	pET-28a	forward: 5′-CCATGGCGATCGGGCCGCCGG-3′ (*Nco*I) reverse: 5′-CTCGAGGTTGCGCGGTGTGGTG-3′ (*Xho*I)
			pGEX-6P-1	N/A (restricted directly from the synthetic construct)
Construct B	Arg^{51}-Asn^{430}		pET-28a	forward: 5′-CCATGGAACGCGGTGCGTGCAG-3′ (*Nco*I) Construct A reverse primer
			pGEX-6P-1	forward: 5′-GGATCCCGCGGTGCGTGCAG-3′ (*BamH*I) Construct A reverse primer
Construct C	Gly^{52}-Leu^{401}		pGEX-6P-1	forward: 5′-GGATCCGGTGCATGTAGCG-3′ (*BamH*I) reverse: 5′-CTCGAGTCACAGCTGCCAGGTC-3′ (*Xho*I)
Construct D	Ser^{57}-Leu^{401}		pGEX-6P-1	forward: 5′-GGATCCGGTGTTATTCCGG-3′ (*BamH*I) Construct C reverse primer
Construct E	Gly^{62}-Leu^{401}		pGEX-6P-1	forward: 5′-GGATCCGGTACAGATCCGG-3′ (*BamH*I) Construct C reverse primer
Construct F	Val^{67}-Leu^{401}		pGEX-6P-1	forward: 5′-GGATCCGTTCCGACCCCGAG-3′ (*BamH*I) Construct C reverse primer
Construct G	Ser^{71}-Leu^{401}	*E. coli* Arctic Express and BL21 (DE3) pLysS	pGEX-6P-1	forward: 5′-GGATCCCAGACCATGCTG-3′ (*BamH*I) Construct C reverse primer
			pCOLD	forward: 5′-CATATGCAGACCATGCTGAATC-3′ (*Nde*I) Construct C reverse primer
Construct H	Leu^{77}-Leu^{401}	*E. coli* BL21 (DE3) pLysS	pGEX-6P-1	forward: 5′-GGATCCCTGCCAGCAGCATG-3′ (*BamH*I) Construct C reverse primer
Construct I	Ile^{24}-Leu^{401}	*E. coli* Origami II and Rosetta gami II	pGEX-6P-1	forward: 5′-GGATCCATTGGTCCGCCTGTTG-3′ (*BamH*I) Construct C reverse primer

*Underlined sequences are restriction sites as indicated in brackets.

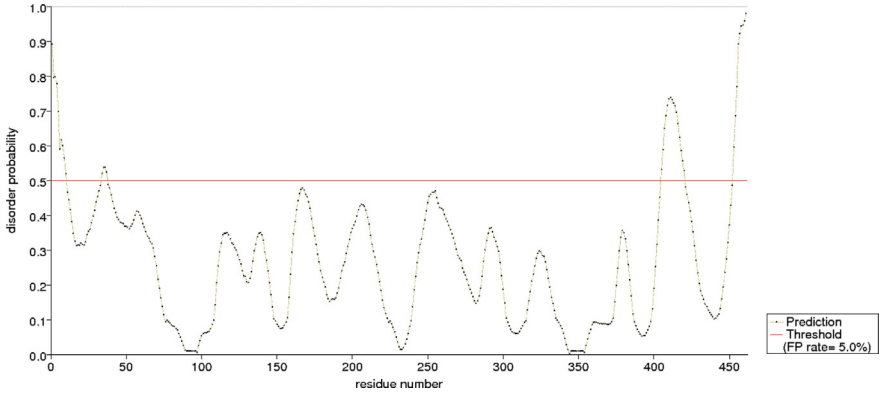

Fig. 2. Disordered region probability plot for *Mtb* H37Rv $MycP_3$ with a prediction false positive rate of 5%, where the disordered region prediction software DrDOS identified two disordered regions, Met^{1}-Pro^{37} and Pro^{405}-E^{461}.

[9,17] making it a potential anti-TB drug target [15,18].

In this study, the gene $mycP_3$ from *M. tuberculosis* H37Rv was cloned and expressed. Extensive effort was made to optimize the construct for soluble mycosin-3 production to increase yield and stability. This report may aid efforts to study mycosin-3 with respect to substrate screening, functional characterization, enzyme kinetics and crystal structure determination.

2. Materials and methods

2.1. Media, plasmids and bacteria strains

Lysogeny broth (LB) was used to culture all *Escherichia coli* strains including XL-1 blue (Promega), BL21 (DE3) pLysS (Promega), Arctic Express (Agilent Technologies), Origami II (Novagen), and Rosetta gami II (Novagen). *E. coli* expression vector pGEX-6P-1

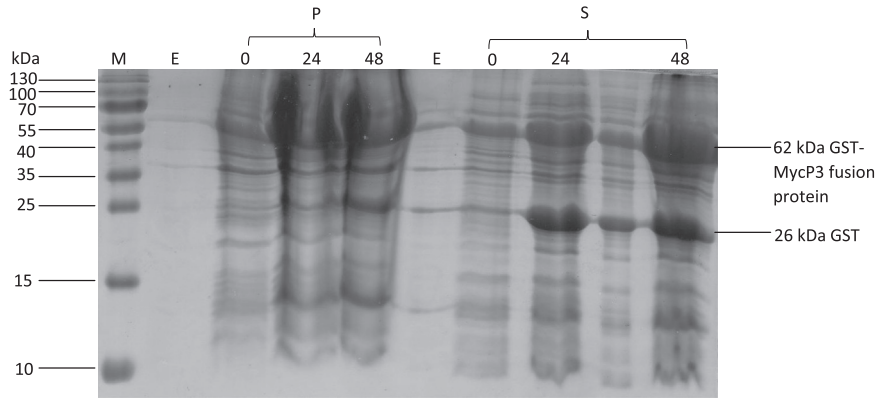

Fig. 3. Test expression and solubility test for Construct G expressed in *E. coli* Arctic Express strain. Protein production level are high in both soluble and insoluble fractions. M: Protein Marker; E: Empty (bands present overflow from other lanes); P: Pellet; S: Supernatant.

Table 2
Sequence identity between mycosin orthologues from *Mtb*, *M. smegmatis*, and *M. thermoresistibile*

SeqA Name	Length	SeqB Name	Length	Alignment Score
Msmeg_0083|$MycP_1$	449	M.therm KEK_05522|$MycP_1$	443	78.8
Mtb Rv3883c|$MycP_1$	446	Msmeg_0083|$MycP_1$	449	72.0
Mtb Rv3883c|$MycP_1$	446	M. therm KEK_05522|$MycP_1$	443	71.1
Mtb Rv0291|$MycP_3$	461	Msmeg_0624|$MycP_3$	459	59.0
Msmeg_0624|$MycP_3$	459	M. therm KEK_05522|$MycP_1$	443	44.0
Mtb Rv3883c|$MycP_1$	446	Msmeg_0624|$MycP_3$	459	44.0
Mtb Rv0291|$MycP_3$	461	M. therm KEK_05522|$MycP_1$	443	43.8
Msmeg_0624|$MycP_3$	459	Msmeg_0083|$MycP_1$	449	43.2
Mtb Rv0291|$MycP_3$	461	Msmeg_0083|$MycP_1$	449	42.8
Mtb Rv0291|$MycP_3$	461	Mtb Rv3883c|$MycP_1$	446	42.4

(GE Health Science), pCOLD (Takara), and pET-28a (Novagen), were used to produce mycosin-3 fusion proteins respectively with an N-terminal glutathione S-transferase (GST)-, an N-terminal His_6-, and a C-terminal His_6-tag.

2.2. Cloning of $MycP_3$ constructs

A range of truncated *mycP*$_3$ constructs were generated by polymerase chain reaction (PCR) using specific primer pairs (Table 1), Phusion DNA polymerase (ThermoScientific), and either *Mtb* H37Rv gemomic DNA (gift from Rob Warren) or codon-optimized *mycP*$_3$ gene (GeneArt) as template. PCR products were ligated into pJET2.1 cloning vector (ThermoScientific) using T4 DNA ligase (Promega). The recombinant pJET2.1 vector was propagated using *E. coli* XL-1 Blue strain and restriction digested to provide an insert for ligation into expression vectors. The recombinant host-specific expression vectors were electroporated into *E. coli* expression host cells.

2.3. Production and purification of $MycP_3$ protein

An overnight 50 mL starter culture was prepared from a single *E. coli* transformant colony. An aliquot of the starter culture was transferred to 1 L LB medium, allowed to grow to mid-log phase ($OD_{600\,nm}$=0.6 to 0.8) at 37 °C and induced with 0.1–0.5 mM isopropyl β-D-1-thiogalactopyranoside (IPTG) at 16, 25 and 30 °C for 18 h for test expression. Arctic express and pCOLD transformants were induced with 0.1 mM IPTG at 13 °C and expression continued for 40 h.

For the GST fusion protein purification, cultures were harvested by centrifugation at 3000*g* at 4 °C for 10 min. The pellet was resuspended in phosphate buffered saline (PBS) and sonicated using a probe sonicator (MSE) at an amplitude of 20 μm for 5 cycles of 30 s with 30 s incubation on ice. The soluble and insoluble fractions of the cell lysate were separated by centrifugation at 14,000*g* at 4 °C for 45 min. The supernatant was agitated with 2 mL PBS-equilibrated glutathione agarose beads (ABT) at 4 °C on a roller mixer for 1 h for fusion protein coupling. The mixture was poured into a drip column and the flowthrough eluted under gravity. The column was washed with 20 column volumes (CV) of PBS. The fusion protein was eluted with elution buffer: 25 mM Tris–HCl, pH 7.4, 150 NaCl, 15 mM reduced glutathione.

For the purification of the His_6-tagged fusion proteins, the *E. coli* cell pellet was resuspended in lysis buffer (25 mM Tris–HCl, pH 7.4, 150 mM NaCl, 10 mM imidazole) and lysed by a tissue and cell homogenizer FastPrep-24 (MP Biomedical) at a speed of 6 m/s for 5 cycles of 30 s alternating with 30 s incubation on ice. The soluble fraction was separated as described above and the target protein was coupled to Ni-NTA beads (Qiagen). The beads were loaded into a drip column and washed with 20 CV wash buffer (25 mM Tris–HCl, pH 7.4, 150 NaCl, 20 mM imidazole) and eluted with elution buffer: wash buffer with 250 mM imidazole.

3. Results

Identifying the catalytic domain of $MycP_3$ is critical prior to cloning and production experiments. $MycP_3$ has a signal peptide, Met^1-Ala^{25}, and an N-terminal extension, Ile^{26}-Gln^{50}, N-terminal of the presumed catalytic domain, Arg^{51}-Leu^{401}, followed by a linker, Pro^{402}-Asn^{430}, and a transmembrane region, Val^{431}-Glu^{461} (Fig. 1). Two truncated constructs of *mycP*$_3$ were amplified from *Mtb* H37Rv genomic DNA and cloned into pET-28a *E. coli* expression vector to produce C-terminally His_6-tagged fusion protein: Construct A encoding Ile^{26}-Asn^{430}, lacks the signal peptide and the transmembrane region. Construct B encodes Arg^{51}-Asn^{430}, which additionally lacks the “pro-peptide” or “N-terminal extension”. Neither construct produced sufficient fusion protein in *E. coli* BL21

(DE3) for visualization on SDS-PAGE.

E. coli codon usage differs significantly from that of mycobacteria [19]. *Mtb mycP*$_3$ DNA encoding Ile^{26}-Asn^{430} was correspondingly codon-harmonized for *E. coli* expression. Corresponding constructs A and B were cloned into plasmid pGEX-6P-1. The encoded GST MycP$_3$ fusion proteins produced small quantities of insoluble protein (Figs. S1 and S2 for construct A). Small amounts of soluble fusion protein proved unstable, prone to rapid proteolysis and precipitation. Chaperone proteins, such as DnaK (69 kDa) and heat shock chaperonin (60 kDa) were co-produced and identified by mass spectrometry (results not shown, service provided by Central Analytical Facility, Stellenbosch University). Triton X-100 treatment removed the chaperones. However, MycP$_3$ was thereupon rapidly degraded (results not shown). Lowering the expression temperature to 16, 25 and 30 °C and varying IPTG concentrations from 0.1 to 1 mM did not improve the solubility or stability of the fusion protein (Fig. S2).

As inherently disordered region (IDR) of the MycP$_3$ fusion protein may limit its solubility and stability, the protein was analysed using PrDOS [20]. This identified Met^1-Pro^{37} and Pro^{405}-E^{461} as potentially disordered (Fig. 2). The region Pro^{402} to Glu^{461} was excluded from analysis as it encompasses the proline-rich linker and the C-terminal transmembrane α-helix [12]. A set of MycP$_3$ constructs removing residues Ile^{26} to Gln^{50} in steps of five to six amino acids was generated: Construct C encodes Gly^{52}-Leu^{401}, D: Ser^{57}-Leu^{401}, E: Gly^{62}-Leu^{401}, F: Val^{67}-Leu^{401}, G: Ser^{71}-Leu^{401}, and H: Leu^{77}-Leu^{401}. The six constructs were cloned into pGEX-6P-1 for GST fusion protein production. Protein production levels for constructs C and D were low while those for E to H were higher (Fig. S3). However, the GST–MycP$_3$ fusion proteins were invariably insoluble (Fig. S4). Gene expression at 16, 25 and 30 °C similarly did not improve the solubility of the resulting protein. Construct G was selected for further optimization of MycP$_3$ production as the elimination of a proline/valine-rich portion (Gly^{52}-Pro^{70}) could improve the yield.

MycP$_3$ contains four cysteines, Cys^{54}, Cys^{123}, Cys^{205} and Cys^{249}. As a secreted protein, MycP$_3$ stability could be disulfide bond dependent. Construct I, encoding MycP$_3$ Ile^{26}-Leu^{401} was produced in *E. coli* expression strains, Origami II and Rosetta Gami II with oxidizing cytosol. However, the resulting protein was again insoluble (results not shown).

The vector pCOLD and the strain Arctic Express are designed to increase the solubility of produced protein [21]. The co-production of pCOLD encoded cold-shock chaperones alongside Construct G did, again, not increase the protein solubility in both BL21 (DE3) and Arctic Express cells (Fig. S5). Unexpectedly, though, expression of Construct G in pGEX-6P-1 vector in Arctic Express produced significant amounts of soluble GST MycP$_3$ Ser^{71}-Leu^{401} fusion protein (Fig. 3) that could be cleaved by PreScission Protease (Roche) to release MycP$_3$ Ser^{71}-Leu^{401} (Fig. S6).

4. Discussion

Production of *Mtb* proteins in *E. coli* has repeatedly been found to be challenging possibly due to its GC rich (> 65%) genome and a distinct codon usage. *Mtb* proteins further incorporate more glycines, alanines, prolines and arginines than *E. coli* and the organism also has post-translational modification machinery that *E. coli* lacks [22]. Although saprophytic *M. smegmatis* is occasionally suitable for *Mtb* protein production, only a handful of successful cases of protein production have been reported [23].

In this study, a range of *mycP*$_3$ constructs were generated with variable truncations and tags. Truncations can eliminate inherently disordered regions whereas a soluble tag may increase the solubility of an attached cargo. Correspondingly, GST–MycP3$_3$ fusion proteins proved more soluble than His$_6$-tagged counterparts. Lower IPTG concentrations and production temperatures limit heat shock protein production, proteolytic degradation, protein aggregation and improve protein stability [24]. MycP$_3$ fusion protein, however, remained insoluble except when produced in Arctic Express. Although rarely used for *Mtb* H37Rv protein production [23], Arctic Express successfully produced GST-tagged MycP$_3$ fusion proteins in significant quantity at low temperature despite lacking an N-terminal extension that stabilizes the catalytic domain [14–16].

The crystal structures of three mycosin orthologues from environmental mycobacterial species with high sequence identity to *Mtb* proteins have been solved. This includes MycP$_1$ from *M. smegmatis* and *M. thermoresistibile*, as well as MycP$_3$ from *M. smegmatis* [14–16]. An amino acid sequence alignment [25] of MycP$_1$ and MycP$_3$ from *Mtb* and *M. smegmatis*, as well as MycP$_1$ from *M. thermoresistibile* reveals that MycP$_1$ from *M. smegmatis* and *M. thermoresistibile* are closely related (alignment score: 78.8) while *Mtb* MycP$_1$ is significantly different (alignment score 72.0) (Table 2). MycP$_3$ from *Mtb* and *M. smegmatis* are even more distantly related. A model for *Mtb* MycP3 was generated using MycP$_3$ from *M. smegmatis* and Swiss Model [26]. The two structures demonstrate no significant differences (Fig. S7). A QMEANZ-score of −1.45 [26], however, indicates some uncertainty in the model structure. The low sequence alignment and QMEANZ-score may indicate a difference in substrate specificity especially as ESX-1 is virulence associated in *Mtb* while it is essential for DNA transfer in *M. smegmatis* [27,28]. Investigating the function of *Mtb* mycosins thus remain important.

To distinguish the enzyme specificity of different mycosins is critical to understand the function of different ESXs. In conclusion, this study reports the successful attempts at producing soluble MycP3 from *Mtb* H37Rv. It is hoped that this information may facilitate future structural and functional studies. Mycosins are evolutionarily only distantly related to other substilisins implying that they could be attractive drug targets especially as MycP$_1$ regulates secretion and processes the secreted virulence factor from ESX-1 whereas MycP$_3$ appears to be involved in iron or possibly even heme acquisition [29].

Author contributions

WS and NG conceived and supervised the study; ZF, WS and NG designed experiments; ZF performed experiments; ZF and WS analysed data; ZF, WS and NG wrote the manuscript.

Acknowledgments

Funding by the National Research Foundation to WDS in the form of Incentive Funding and Competitive Funding CPRR13092045495 are gratefully acknowledged.

Appendix A. Supplementary material

Supplementary data associated with this article can be found in the online version at http://dx.doi.org/10.1016/j.bbrep.2016.02.005.

References

[1] B.B. Finlay, S. Falkow, Common themes in microbial pathogenicity revisited, Microbiol. Mol. Biol. Rev. 61 (2) (1997) 136–169.
[2] N.C. Gey Van Pittius, J. Gamieldien, W. Hide, G.D. Brown, R.J. Siezen, A. D. Beyers, The ESAT-6 gene cluster of Mycobacterium tuberculosis and other high G+C Gram-positive bacteria, Genome Biol. 2 (10) (2001), RESEARCH0044.

[3] A.M. Abdallah, N.C. Gey van Pittius, P.A.D. Champion, J. Cox, J. Luirink, C.M.J. E. Vandenbroucke-Grauls, et al., Type VII secretion—mycobacteria show the way, Nat. Rev. Microbiol. 5 (11) (2007) 883–891.
[4] N.C. Gey van Pittius, S.L. Sampson, H. Lee, Y. Kim, P.D. van Helden, R.M. Warren, Evolution and expansion of the Mycobacterium tuberculosis PE and PPE multigene families and their association with the duplication of the ESAT-6 (esx) gene cluster regions, BMC Evol. Biol. 6 (2006) 95.
[5] E.N.G. Houben, K.V. Korotkov, W. Bitter, Take five – type VII secretion systems of mycobacteria, Biochim Biophys. Acta (2013).
[6] M.S. Siegrist, M. Steigedal, R. Ahmad, A. Mehra, M.S. Dragset, B.M. Schuster, et al., Mycobacterial esx-3 requires multiple components for iron acquisition, mBio 5 (2014) 3.
[7] M.S. Siegrist, M. Unnikrishnan, M.J. McConnell, M. Borowsky, T.-Y. Cheng, N. Siddiqi, et al., Mycobacterial Esx-3 is required for mycobactin-mediated iron acquisition, Proc. Natl. Acad. Sci. USA 106 (44) (2009) 18792–18797.
[8] L.S. Ates, R. Ummels, S. Commandeur, R. van der Weerd, M. Sparrius, E. Weerdenburg, et al., Essential role of the ESX-5 secretion system in outer membrane permeability of pathogenic Mycobacteria, PLoS Genet. 11 (5) (2015) e1005190.
[9] J.E. Griffin, J.D. Gawronski, M.A. Dejesus, T.R. Ioerger, B.J. Akerley, C.M. Sassetti, High-resolution phenotypic profiling defines genes essential for mycobacterial growth and cholesterol catabolism, PLoS Pathog. 7 (9) (2011) e1002251.
[10] C.M. Sassetti, D.H. Boyd, E.J. Rubin, Genes required for mycobacterial growth defined by high density mutagenesis, Mol. Microbiol. 48 (1) (2003) 77–84.
[11] E.N.G. Houben, J. Bestebroer, R. Ummels, L. Wilson, S.R. Piersma, C.R. Jiménez, et al., Composition of the type VII secretion system membrane complex, Mol. Microbiol. 86 (2) (2012) 472–484.
[12] G.D. Brown, J.A. Dave, N.C. Gey van Pittius, L. Stevens, M.R. Ehlers, A.D. Beyers, The mycosins of Mycobacterium tuberculosis H37Rv: a family of subtilisin-like serine proteases, Gene 254 (1–2) (2000) 147–155.
[13] Y.M. Ohol, D.H. Goetz, K. Chan, M.U. Shiloh, C.S. Craik, J.S. Cox, Mycobacterium tuberculosis MycP1 protease plays a dual role in regulation of ESX-1 secretion and virulence, Cell Host Microbe 7 (3) (2010) 210–220.
[14] M. Solomonson, P.F. Huesgen, G.A. Wasney, N. Watanabe, R.J. Gruninger, G. Prehna, et al., Structure of the mycosin-1 protease from the Mycobacterial ESX-1 protein type VII secretion system, J. Biol. Chem. 288 (24) (2013) 17782–17790.
[15] J.M. Wagner, T.J. Evans, J. Chen, H. Zhu, E.N.G. Houben, W. Bitter, et al., Understanding specificity of the mycosin proteases in ESX/type VII secretion by structural and functional analysis, J. Struct. Biol. 184 (2) (2013) 115–128.
[16] D. Sun, Q. Liu, Y. He, C. Wang, F. Wu, C. Tian, et al., The putative propeptide of MycP1 in mycobacterial type VII secretion system does not inhibit protease activity but improves protein stability, Protein Cell 4 (12) (2013) 921–931.
[17] C.M. Sassetti, D.H. Boyd, E.J. Rubin, Genes required for mycobacterial growth defined by high density mutagenesis, Mol. Microbiol. 48 (1) (2003) 77–84.
[18] M.S. Frasinyuk, S. Kwiatkowski, J.M. Wagner, T.J. Evans, R.W. Reed, K. V. Korotkov, et al., Pentapeptide boronic acid inhibitors of Mycobacterium tuberculosis MycP1 protease, Bioorg. Med. Chem. Lett. (2014).
[19] C. Scapoli, E. Bartolomei, S. De Lorenzi, A. Carrieri, G. Salvatorelli, A. Rodriguez-Larralde, et al., Codon and aminoacid usage patterns in Mycobacteria, J. Mol. Microbiol. Biotechnol. 17 (2) (2009) 53–60.
[20] T. Ishida, K. Kinoshita, PrDOS: prediction of disordered protein regions from amino acid sequence, Nucleic Acids Res. 35 (Web Server issue) (2007) W460–W464.
[21] K. Hayashi, C. Kojima, pCold-GST vector: a novel cold-shock vector containing GST tag for soluble protein production, Protein Expr. Purif. 62 (1) (2008) 120–127.
[22] S. Daugelat, J. Kowall, J. Mattow, D. Bumann, R. Winter, R. Hurwitz, et al., The RD1 proteins of Mycobacterium tuberculosis: expression in Mycobacterium smegmatis and biochemical characterization, Microbes Infect.: Inst. Pasteur 5 (12) (2003) 1082–1095.
[23] Z. Fang, R.G. van der Merwe, R.M. Warren, W.-D. Schubert, N.C. Gey van Pittius, Assessing the progress of Mycobacterium tuberculosis H37Rv structural genomics, Tuberculosis 95 (2) (2015) 131–136.
[24] R.S. Donovan, C.W. Robinson, B.R. Glick, Review: optimizing inducer and culture conditions for expression of foreign proteins under the control of the lac promoter, J. Ind. Microbiol. 16 (3) (1996) 145–154.
[25] M.A. Larkin, G. Blackshields, N.P. Brown, R. Chenna, P.A. McGettigan, H. McWilliam, et al., Clustal W and Clustal X version 2.0, Bioinformatics 23 (21) (2007 1) 2947–2948.
[26] P. Benkert, M. Biasini, T. Schwede, Toward the estimation of the absolute quality of individual protein structure models, Bioinformatics 27 (3) (2011) 343–350.
[27] A. Coros, B. Callahan, E. Battaglioli, K.M. Derbyshire, The specialized secretory apparatus ESX-1 IS essential for DNA transfer in Mycobacterium smegmatis, Mol. Microbiol. 69 (4) (2008) 794–808.
[28] J.L. Flint, J.C. Kowalski, P.K. Karnati, K.M. Derbyshire, The RD1 virulence locus of Mycobacterium tuberculosis regulates DNA transfer in Mycobacterium smegmatis, Proc. Natl. Acad. Sci. USA 101 (34) (2004) 12598–12603.
[29] Z. Fang, S.L. Sampson, R.M. Warren, N.C. Gey van Pittius, M. Newton-Foot, Iron acquisition strategies in mycobacteria, Tuberculosis 95 (2) (2015) 123–130.